

# Methane-derived hydrocarbons produced under upper-mantle conditions

Anton Kolesnikov<sup>1,2</sup>, Vladimir G. Kutcherov<sup>2,3</sup> and Alexander F. Goncharov<sup>1\*</sup>

There is widespread evidence that petroleum originates from biological processes<sup>1–3</sup>. Whether hydrocarbons can also be produced from abiogenic precursor molecules under the high-pressure, high-temperature conditions characteristic of the upper mantle remains an open question. It has been proposed that hydrocarbons generated in the upper mantle could be transported through deep faults to shallower regions in the Earth's crust, and contribute to petroleum reserves<sup>4,5</sup>. Here we use *in situ* Raman spectroscopy in laser-heated diamond anvil cells to monitor the chemical reactivity of methane and ethane under upper-mantle conditions. We show that when methane is exposed to pressures higher than 2 GPa, and to temperatures in the range of 1,000–1,500 K, it partially reacts to form saturated hydrocarbons containing 2–4 carbons (ethane, propane and butane) and molecular hydrogen and graphite. Conversely, exposure of ethane to similar conditions results in the production of methane, suggesting that the synthesis of saturated hydrocarbons is reversible. Our results support the suggestion that hydrocarbons heavier than methane can be produced by abiogenic processes in the upper mantle.

The speciation of carbon in the Earth's interior is critical for understanding the origin of petroleum<sup>6</sup>. Formation and stability of methane under conditions corresponding to the Earth's upper mantle have been demonstrated in recent years<sup>6–9</sup> but the formation of heavier alkanes remains unclear and controversial. Shock-wave experiments<sup>10,11</sup> suggest the decomposition of methane into molecular H<sub>2</sub> and carbon, with precipitation of diamond<sup>12</sup>. In contrast, theoretical calculations<sup>13,14</sup> indicate the presence of saturated hydrocarbons before complete dissociation into diamond and hydrogen. Earlier diamond anvil cell (DAC) experiments<sup>15–19</sup> do not support the formation of alkanes, and rather indicate the dissociation of methane to atomic carbon in the form of diamond<sup>16,17</sup> or soot<sup>15,18</sup> and molecular hydrogen<sup>17,18</sup> and also the presence of unidentified hydrocarbons<sup>16,18,19</sup>. Ethane synthesis was recently demonstrated in laser-heated DAC experiments on methane above 1,200 K at pressures higher than 10 GPa (ref. 20). Motivated by previous experimental work and theoretical predictions, we experimentally studied the stability of methane and ethane under the pressure–temperature (*P–T*) and oxidation-state conditions representative of the Earth's upper mantle.

We carried out our experiments in a symmetric laser-heated DAC (see details in the Methods section; Fig. 1). Our experiments combined *in situ* Raman measurements in a laser spot or its vicinity and Raman microprobe studies (combined with X-ray diffraction in the case of oxidized conditions) of the products quenched to room temperature. Several experiments at varying *P–T* conditions using different materials (used to engineer the laser-heating experiment) were carried out to study their effects on the sample chemistry (see Supplementary Table S1).

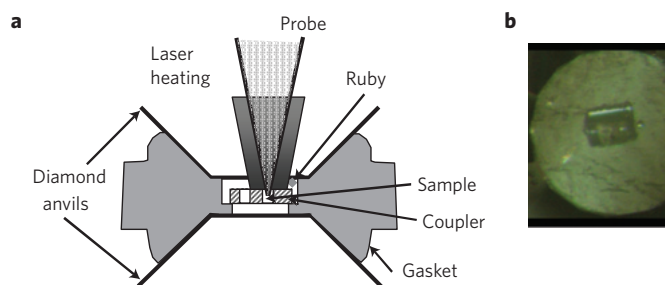


**Figure 1 | Laser-heating experiment.** **a**, Schematic diagram of the sample arrangement in a DAC cavity. **b**, Microphotograph of a DAC cavity before heating.

The Raman spectra at elevated temperatures show only minor changes below 900 K; on heating to a higher temperature, a new peak appears at about 1,000 cm<sup>-1</sup> (Fig. 2a), corresponding to ethane. If heated to 1,500 K and higher, a set of lines corresponding to molecular hydrogen becomes clearly observable (see Supplementary Information). At this point, the Raman signal from methane is substantially reduced; in the same spectral range, a new band appears corresponding to atomic carbon (Fig. 2a).

The Raman spectra of the quenched sample show a diversity of various products depending on the highest temperature to which the sample was exposed (Fig. 2b). The Raman signal from methane remains in all spectra, but it is substantially diminished in the areas subjected to the highest temperatures. In the laser spot, the highest temperature was approximately 2,500 K; temperatures in two other less heated areas can be estimated as 1,600 and 900 K, respectively. The most heated area shows a very large fluorescence and a broad high-frequency peak at 4,300 cm<sup>-1</sup>, which can be attributed to hydrogen–methane compounds<sup>21</sup>. In addition, Raman signals at 1,600 and 2,800 cm<sup>-1</sup>, clear characteristics of graphite, were observed in the two most heated sample areas. The hydrocarbon reaction products can be seen most clearly in less heated areas (position 3). The reaction products remain present without substantial change in the timescale of hours, but their Raman signatures become weaker after several days, probably as the result of diffusion away from the reaction zone. The reaction products do not decompose with changing pressure either up (to 14 GPa) or down to ambient pressure.

The Raman spectra of the quenched sample in the area richest in reaction products (Fig. 2c) show Raman signals of molecular hydrogen, graphite and saturated hydrocarbons. The last of these include ethane (mostly) and (to a lesser extent) propane and butane. These hydrocarbon products have very distinct Raman bands in the region of the skeletal C–C stretching (780–1,200 cm<sup>-1</sup>) and C–H bending modes (1,400–1,600 cm<sup>-1</sup>),

<sup>1</sup>Geophysical Laboratory, Carnegie Institution of Washington, Washington, District of Columbia 20015, USA, <sup>2</sup>Lomonosov Moscow State Academy of Fine Chemical Technology, 117571 Moscow, Russia, <sup>3</sup>Royal Institute of Technology, SE-100 44 Stockholm, Sweden. \*e-mail: goncharov@gl.ciw.edu.

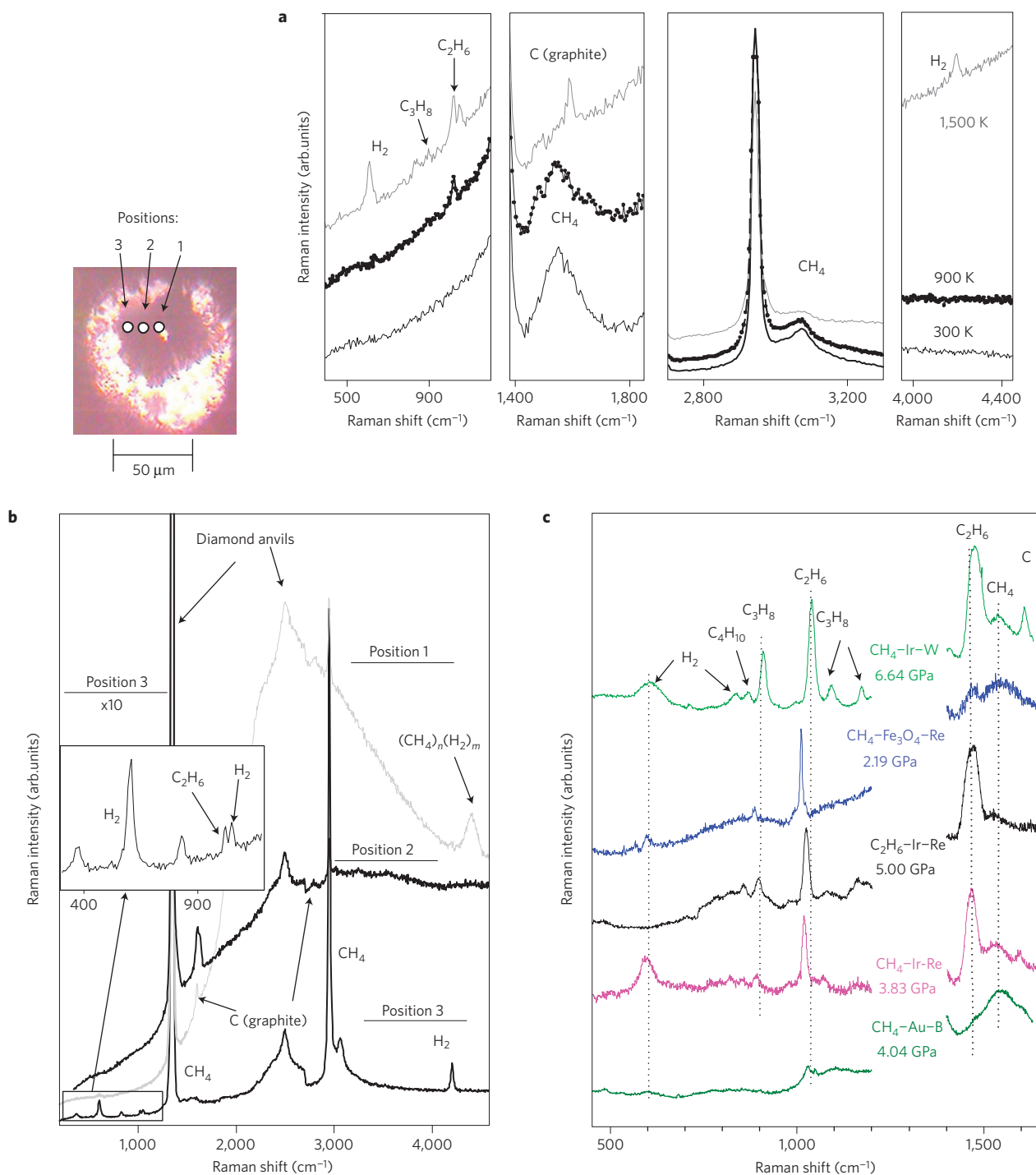
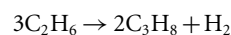


**Figure 2 | Representative Raman spectra.** **a**, The temperature dependence of methane at 2 GPa. **b**, The quenched sample after heating at 2.5 GPa to the maximum temperature of 2,500 K. The inset microphotograph shows the probed positions (dots); the Raman spectra are shown in the respective positions. Position 1 corresponds to the heating spot. **c**, The reaction products quenched after heating at various pressures. Precursors and materials that were used to make couplers and gaskets are listed. Vertical lines are drawn as guides to the eye to trace the spectral lines corresponding to the reaction products.

which allows definite identification of the reaction products (see Supplementary Table S2). No other reaction products were observed (such as, unsaturated hydrocarbons), which would be easily distinguishable because they have very distinct Raman spectra owing to the presence of doubly and triply bonded carbon.

Laser-heating experiments with pure ethane as a precursor up to 1,500 K and 5 GPa (using an Ir coupler) again yield a variety of saturated hydrocarbon products (propane, butane and methane) and elemental carbon, whereas no hydrogen could

be detected (Fig. 2c, see also Supplementary Fig. S1). This is consistent with the following reaction paths, which create propane (and similar reactions that create heavier hydrocarbons) and methane:



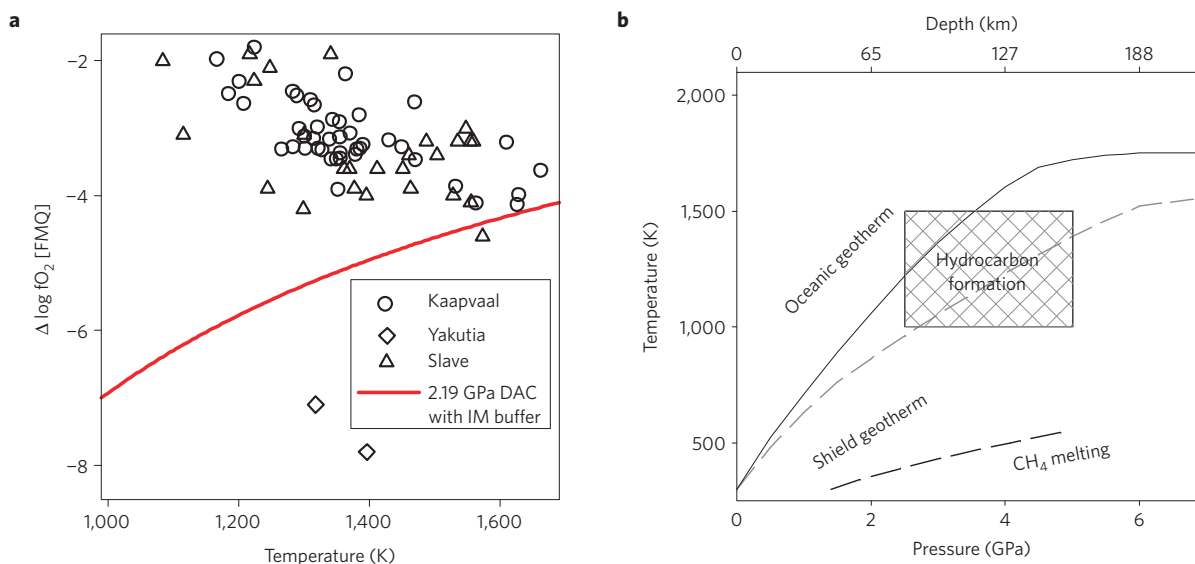


**Figure 3 | P-T- $f_{O_2}$  conditions in our DAC experiments and in the upper mantle. a**,  $f_{O_2}$  conditions of the laser-heating experiment with the IM buffer (calculated using ref. 22) in comparison with the redox profile of Kaapvaal craton, South Africa<sup>26</sup>, Slave craton<sup>27</sup> and Yakutian craton<sup>28</sup>.

**b**, Pressure-temperature range corresponding to hydrocarbon formation in laser-heating experiments in comparison with the model oceanic (60 mW m<sup>-2</sup>) and shield (40 mW m<sup>-2</sup>) geotherms<sup>29</sup> and the methane melting line<sup>25</sup>.

As in the case of methane, the presence of elemental carbon as the reaction product indicates that other reaction paths are also possible (such as decomposition). Nevertheless, it is remarkable that methane was generated as the product of these reactions. The reversibility of the methane-ethane reaction under high  $P$ - $T$  conditions suggests that synthesis of saturated hydrocarbons follows the thermodynamic (equilibrium) path as was predicted earlier<sup>7</sup>. Moreover, given that graphite and hydrogen react to form methane under similar conditions (Sharma, Cody and Hemley, unpublished), the decomposition of methane into carbon and hydrogen (Fig. 2a) also has a reversible character that may correspond to an equilibrium process in the Earth's interiors.

To study the effect of the mantle redox environment on the chemical reactivity of methane, we positioned a 5- $\mu$ m-thick plate of single-crystal magnetite ( $Fe_3O_4$ ) and used it as a coupler. We find that magnetite (which was heated directly by a laser, and, therefore, was hot) reacts with methane at high temperatures, thereby providing oxidizing conditions in the hot area of the sample cavity. Raman and X-ray diffraction probes of the quenched materials show that the reaction products include metallic iron, carbon in diamond and graphite forms, and water ice (Fig. 2c and Supplementary Figs S2-S4), which is consistent with the net reaction path  $Fe_3O_4 + 2CH_4 \rightarrow 3Fe + 2C + 4H_2O$ . Neither  $CO_2$ , nor CO was detected. As both magnetite and Fe were present in the reaction chamber for the duration of the experiment (verified by the presence of a small amount of  $Fe_3O_4$  after the reaction), we conjecture that they form a redox buffer (Fe- $Fe_3O_4$ , IM, ref. 22), which determines the oxygen fugacity ( $f_{O_2}$ ; Fig. 3a) in the sample cavity. The values of  $f_{O_2}$  determined with respect to a common quartz-fayalite-magnetite buffer are probably close to some reduced environments observed below cratons in the Earth's mantle (Fig. 3a). The Raman results (Fig. 2c) show that oxidation conditions in the cavity do not change the chemistry of the methane transformation process principally. We find ethane, water, molecular hydrogen and carbon in diamond and graphite forms (in more heated regions), and also molecular hydrogen (in less heated regions) as the reaction products (Fig. 2c).

To study possible catalytic effects of the formation of hydrocarbons, we carried out several laser-heating experiments using various

materials for couplers and gaskets. As the heating spot was normally away from the gasket, we did not expect any catalytic effects related to its presence. Indeed, changing the gasket material from tungsten to rhenium did not affect the results of the experiment. In the next experiment, we used compressed amorphous boron as a coupler and also introduced a gold liner into the rhenium gasket. Only hydrogen and graphite could be seen after the heating at 2 GPa, and no hydrocarbons could be detected. We again detected the Raman spectrum of ethane in the laser-heated methane when the pressure had been increased to 4 GPa. This shows that the effect of pressure is essential for the observed reaction. In addition, we find that the duration of the experiments (10 s to minutes) does not change the reaction yield as long as the critical temperature has been reached. This is consistent with the observed equilibrium character of the process and suggests that no catalyst is needed. However, the presence of iridium and other materials may have some catalytic effect in our experiments, lowering the temperature needed for the reaction to proceed and increasing the yield. Given the great variety of chemical environments in the upper mantle, catalysis may occur and have an important role in methane transformation on the geological timescale.

Previous laser-heating experiments<sup>15-18</sup> are in agreement with our observations, in that the methane dissociated into carbon and hydrogen, but the formation of saturated hydrocarbons was not detected, most probably because the temperature could not be controlled accurately enough. Owing to the use of a laser-heating technique with a metallic coupler (Fig. 1), we could heat larger volumes more uniformly in more controllable conditions than previously. This enabled us to obtain larger amounts of reaction products, sufficient for conclusive analysis using our micro-Raman probe. Our results are also in agreement with the previous theoretical calculations<sup>13,14</sup>, in that the formation of hydrocarbons occurs at less extreme conditions than the dissociation to carbon and hydrogen, although we find it at much lower pressures.

The experimental conditions under which we carry out the synthesis of  $C_2$ - $C_4$  alkanes are consistent with the pressure-temperature conditions in the Earth's mantle at the depth of 70-150 km (Fig. 3b). Increased oxygen fugacity conditions do not substantially affect the hydrocarbon formation (Fig. 3a). This suggests an extended stability of reduced forms of carbon (including

elemental carbon, such as, diamond). The formation of methane<sup>6,9</sup> and even heavier alkanes<sup>7</sup> by chemical reaction of carbonate, FeO and water, was demonstrated to occur at similar pressure–temperature conditions as in our experiments. Our work proposes a chemical transformation path that can explain the formation of hydrocarbons in the deep Earth. Unlike the previous study (ref. 7), where only the quenched reaction products could be examined, we show here that heavier alkanes can be formed directly from methane without the presence of any other materials (such as catalysts), even under the redox conditions representative of the Earth's mantle conditions. Moreover, our data show that two chemical transformations compete under these conditions; the second involves the dissociation of methane to molecular hydrogen and graphite. We argue that the formation of hydrogen and its subsequent oxidation may create favourable reducing conditions for the formation of hydrocarbons<sup>7</sup> and further assist their migration to shallow depths. Migration of hydrogen-bearing fluid upwards may create reduced channels in the weak zones of the lithosphere and prevent hydrocarbon oxidation during its ascent. The contribution of this abiogenic mechanism to hydrocarbon accumulation in major petroleum deposits found in active subcontinental settings of craton margins and rift zones could be actively searched in the future.

A number of chemical reactions have previously been considered (for example, ref. 23) as a potential mechanism for hydrocarbon genesis, but they were not verified experimentally under conditions relevant to the Earth's interior. Our study determines that experimental *P–T* conditions of hydrocarbon synthesis are appropriate for the Earth's mantle (Fig. 3), creating the possibility of the abiogenic synthesis of petroleum components in the Earth's upper mantle.

## Methods

Methane (99.9995%) and ethane (99.9%) were loaded in the gas phase at high pressure (0.2 GPa) into the cavity of a symmetric DAC equipped with low-fluorescence anvils with 0.3-mm-diameter flat culet. We used a custom Raman spectrometer combined with a laser-heating system for high- and room-temperature Raman and radiometric temperature measurements. We used the 458 nm line of a 100 mW Ar ion laser to excite the Raman spectra. A Mitutoyo near-infrared  $\times 20$  long-working-distance objective lens was used for the collection of Raman spectra in the backscattering geometry. The Raman spectra were collected with the 460-mm-focal-length *f*/5.3 imaging spectrograph equipped with two 1,500 and 300 grooves  $\text{mm}^{-1}$  gratings on the same turret. This feature allows one to first take a quick exploratory spectrum over a wide spectral range ( $-4,000$  to  $4,000 \text{ cm}^{-1}$  in one spectral window) and then study regions of interest with higher accuracy and resolution. The YLF laser radiation was introduced into the Raman system using polarizing beam-splitter cubes and was focused to a 20–25  $\mu\text{m}$  spot using the same objective lens. Controlled attenuation of the YLF beam was achieved using a combination of a polarizing beam-splitter cube and a  $\lambda/2$  wave plate. To provide efficient heat transfer to the sample, we placed a  $80 \times 50 \times 12 \mu\text{m}$  plate (coupler) with several holes of approximately 10  $\mu\text{m}$  diameter into the gasket cavity. These holes formed a sample cavity with reduced temperature gradients for *in situ* Raman measurements. We used various materials for gaskets and couplers. These include the creation of redox conditions and the study of possible catalytic effects. It should be noted that gasket and diamond anvils stay cold (close to room temperature) during the laser-heating experiments because of their much larger thermal conductivity compared with the sample.

To provide mechanical stability of the coupler during heating (methane melts in the pressure range of interest), we made a recess in the gasket hole and positioned the coupler inside (Fig. 1). As the heating laser spot is much smaller than the coupler (approximately 20  $\mu\text{m}$  in diameter), large temperature gradients are generated across the coupler during the heating, ranging from the highest (up to 2,500 K in selected experiments) to near room temperature at the point of contact with the gasket. These temperature gradients produce a variety of temperature conditions for the sample. Nevertheless, given the duration of the experiment ( $> 10 \text{ s}$ ) and a temperature stability during the laser heating, we believe that chemical and temperature equilibria have been reached locally in every spatial point of the sample. No qualitative changes in spectra were detected between quenched and high-temperature measurements. Thus, measurements of the samples quenched to room temperature are representative for the high-temperature chemical reactivity. No hydrocarbons were detected by Raman measurements on the gasket before loading and after laser-heating experiments.

The Raman spectra of methane at 3–6 GPa show  $\nu_1$ ,  $\nu_2$  and  $\nu_3$  fundamentals corresponding to symmetric stretching, symmetric bending and antisymmetric stretching modes, respectively (Fig. 2a, also see Supplementary Table S2 for the mode assignment in reagents and reaction products). We carried out separate pressure runs at 300 K for ethane and propane to establish the pressure dependence of the vibrational modes (see Supplementary Information); the Raman modes of butane were assumed to shift with pressure similarly. The results allowed us to carry out unambiguous identification of the hydrocarbon reaction products.

Experimental temperature scans were carried out near-isobarically in the pressure range from 2 to 14.1 GPa. Pressure was determined at room temperature using a conventional ruby manometer before and after laser heating (which was the same within the experimental error in most cases). Temperature and pressure gradients were estimated by several techniques. The maximum coupler temperature was determined radiometrically by fitting the Planck function to the thermal radiation emitted. In several cases, the Raman Stokes-to-anti-Stokes intensity technique (for example, ref. 24) was used to determine the temperature of methane away from the heating spot. As a guide, we could also estimate the temperature by observing the appearance of the molten methane vesicle near the heated coupler using the melting line measurements<sup>25</sup>. On one occasion, we used the Raman spectrum of a  $^{13}\text{C}$  gauge pressed into the coupler to determine the pressure (from the frequency shift) and temperature (Stokes-to-anti-Stokes intensity) *in situ*. The results were consistent with other techniques and indicated very little pressure change on heating to approximately 900 K.

Received 8 September 2008; accepted 30 June 2009;  
published online 26 July 2009

## References

- Tissot, B. P. & Welte, D. H. *Petroleum Formation and Occurrence* (Springer, 1984).
- Whiticar, M. J., Faber, E. & Schoell, M. Biogenic methane formation in marine and freshwater environments:  $\text{CO}_2$  reduction vs acetate fermentation—*isotope evidence*. *Geochim. Cosmochim. Acta* **50**, 693–709 (1986).
- Schoell, M. Multiple origins of methane in the earth. *Chem. Geol.* **71**, 1–10 (1988).
- Porfir'ev, V. B. Inorganic origin of petroleum. *Am. Assoc. Petrol. Geol. Bull.* **58**, 3–33 (1974).
- Krayushkin, V. A. Oil and gas fields of the abyssal genesis. *D. I. Mendeleev J. All-Union. Chem. Soc.* **31**, 241–252 (1986).
- Scott, H. P., Hemley, R. J. & Mao, H. *et al.* Generation of methane in the Earth's mantle: *In situ* high pressure–temperature measurements of carbonate reduction. *Proc. Natl Acad. Sci. USA* **101**, 14023–14026 (2004).
- Kenney, J. F., Kutcherov, V. G., Bendeliani, N. A. & Alekseev, V. A. The evolution of multicomponent systems at high pressures: VI. The thermodynamic stability of the hydrogen–carbon system: The genesis of hydrocarbons and the origin of petroleum. *Proc. Natl Acad. Sci. USA* **99**, 10976–10981 (2002).
- Kutcherov, V. G., Bendeliani, N. A., Alekseev, V. A. & Kenney, J. F. Synthesis of hydrocarbons from minerals at pressures up to 5 GPa. *Dokl. Akad. Nauk [in Russian]* **387**, 789–792 (2002).
- Chen, J. Y., Jin, L. J., Dong, J. P., Zheng, H. F. & Liu, G. Y. Methane formation from  $\text{CaCO}_3$  reduction catalyzed by high pressure. *Chin. Chem. Lett.* **19**, 475–478 (2008).
- Nellis, W. J., Ree, F. H., Thiel, M. Van & Mitchell, A. C. Shock compression of liquid carbon monoxide and methane to 90 GPa (900 kbar). *J. Chem. Phys.* **75**, 3055–3063 (1981).
- Nellis, W. J., Hamilton, D. C. & Mitchell, A. C. Electrical conductivities of methane, benzene, and polybutene shock compressed to 60 GPa (600 kbar). *J. Chem. Phys.* **115**, 1015–1019 (2001).
- Ross, M. The ice layer in Uranus and Neptune—diamonds in the sky. *Nature* **292**, 435–436 (1981).
- Ancilotto, F., Chiarotti, G. L., Scandolo, S. & Tosatti, E. Dissociation of methane into hydrocarbons at extreme (planetary) pressure and temperature. *Science* **275**, 1288–1290 (1997).
- Kress, J. D., Bickham, S. R., Collins, L. A., Holian, B. L. & Goedecker, S. Tight-binding molecular dynamics of shock waves in methane. *Phys. Rev. Lett.* **83**, 3896–3899 (1999).
- Culler, T. S. & Schiferl, D. New chemical reactions in methane at high temperatures and pressures. *J. Phys. Chem.* **97**, 703–706 (1993).
- Benedetti, L. R. *et al.* Dissociation of  $\text{CH}_4$  at high pressures and temperatures: Diamond formation in giant planet interiors. *Science* **286**, 100–102 (1999).
- Zerr, A., Serghiou, G., Boehler, R. & Ross, M. Decomposition of alkanes at high pressure and temperatures. *High Press. Res.* **26**, 23–32 (2006).
- Hemley, R. J. & Mao, H. K. in *Proc. 13th APS Conf. on Shock-compression of Condensed Matter* (eds Furnish, M. D., Gupta, Y. M. & Forbes, J. W.) 17–26 (AIP, 2004).
- Chen, J. Y., Jin, L. J., Dong, J. P. & Zheng, H. F. *In situ* Raman spectroscopy study on dissociation of methane at high temperatures and at high pressures. *Chin. Phys. Lett.* **25**, 780–782 (2008).

20. Hirai, H., Konagai, K., Kawamura, T., Yamamoto, Y. & Yagi, T. Polymerization and diamond formation from melting methane and their implications in ice layer of giant planets. *Phys. Earth Planet. Inter.* **174**, 242–246 (2009).
21. Somayazulu, M. S., Finger, L. W., Hemley, R. J. & Mao, H. K. High-pressure compounds in methane–hydrogen mixtures. *Science* **271**, 1400–1402 (1996).
22. Huebner, J. S. in *Research Techniques for High Pressure and High Temperature* (ed. Ulmer, G. C.) 123–177 (Springer, 1972).
23. Sherwood Lollar, B. S. *et al.* Unravelling abiogenic and biogenic sources of methane in the Earth's deep subsurface. *Chem. Geol.* **226**, 328–339 (2006).
24. Goncharov, A. F. *et al.* Dynamic ionization of water under extreme conditions. *Phys. Rev. Lett.* **94**, 125508 (2005).
25. Yagi, T. & Suzuki, H. Melting curve of methane to 4.8 GPa determined by the Ruby pressure–temperature marker. *Proc. Japan Acad. Ser. B* **66**, 167–172 (1990).
26. Woodland, A. B. & Koch, M. Variation in oxygen fugacity with depth in the upper mantle beneath the Kaapvaal craton, Southern Africa. *Earth. Planet. Sci. Lett.* **214**, 295–310 (2003).
27. McCammon, C. & Kopylova, M. G. A redox profile of the Slave mantle and oxygen fugacity control in the cratonic mantle. *Contrib. Mineral. Petrol.* **148**, 55–68 (2004).
28. Simakov, S. K. Redox state of eclogites and peridotites from sub-cratonic upper mantle and a connection with diamond genesis. *Contrib. Mineral. Petrol.* **151**, 282–296 (2006).
29. Pollack, H. N. & Chapman, D. S. On the regional variation of heat flow, geotherms, and lithospheric thickness. *Tectonophysics* **38**, 279–296 (1977).

## Acknowledgements

We thank K. Litasov, Y. Fei, J. C. Crowhurst, M. Somayazulu, V. Struzhkin, R. Cohen, D. Foustoukos, J. Montoya, T. Strobel and R. J. Hemley for valuable information, comments and discussions. We thank S. Sinogeikin for help with X-ray diffraction experiments. A.K. acknowledges the support from INTAS through YSF Ref. No. 06-1000014-6546. V.G.K. acknowledges the support from INTAS Ref. No. 06-1000013-8750. We acknowledge support by the US Department of Energy (DOE)/National Nuclear Security Agency through the Carnegie/DOE Alliance Center, NSF- EAR, the W. M. Keck Foundation and the Carnegie Institution of Washington. Use of the HPCAT facility (Carnegie Institution of Washington) was supported by DOE-BES, DOE-NNSA (CDAC), NSF, DOD–TACOM and the W. M. Keck Foundation. Use of the Advanced Photon Source was supported by the US Department of Energy, Office of Science, Office of Basic Energy Sciences, under Contract No. W-31-109-Eng-38.

## Author contributions

V.G.K. designed the study. A.F.G. and A.K. designed the experiments. A.K. and A.F.G. carried out the experiments and reduced the data. A.K. carried out the data analysis. A.F.G. wrote the manuscript with substantial contributions made by the other authors. All authors discussed the results and implications and commented on the manuscript at all stages.

## Additional information

Supplementary information accompanies this paper on [www.nature.com/naturegeoscience](http://www.nature.com/naturegeoscience). Reprints and permissions information is available online at <http://npg.nature.com/reprintsandpermissions>. Correspondence and requests for materials should be addressed to A.F.G.